doi:10.1093/jmcb/mjy011
Published online February 19, 2018

Article

BMP4 facilitates beige fat biogenesis via regulating adipose tissue macrophages

Shu-Wen Qian†, Meng-Yuan Wu†, Yi-Na Wang, Ya-Xin Zhao, Ying Zou, Jia-Bao Pan, Yan Tang, Yang Liu, Liang Guo, and Qi-Qun Tang*

Key Laboratory of Metabolism and Molecular Medicine, The Ministry of Education; Department of Biochemistry and Molecular Biology, Fudan University Shanghai Medical College, Shanghai 200032, China
† These authors contributed equally to this work.
* Correspondence to: Qi-Qun Tang, E-mail: qqtang@shmu.edu.cn

Edited by Feng Liu

Thermogenic beige fat improves metabolism and prevents obesity. Emerging evidence shows that the activation of M2 macrophages stimulates beige adipogenesis, whereas the activation of M1 macrophages, which play a major role in inflammation, impedes beige adipogenesis. Thus, the identification of factors that regulate adipose tissue macrophages (ATMs) will help clarify the mechanism involved in beiging. Here, we found that one of the secreted proteins in adipose tissue, namely, BMP4, alters the ATM profile in subcutaneous adipose tissue by activating M2 and inhibiting M1 macrophages. Mechanistically, the BMP4-stimulated p38/MAPK/STAT6/PI3K–AKT signalling pathway is involved. Meanwhile, BMP4 improved the potency of M2 macrophages to induce beige fat biogenesis. Considering that the overexpression of BMP4 in adipose tissue promotes the beiging of subcutaneous adipose tissue and improves insulin sensitivity, these findings provide evidence that BMP4 acts as an activator of beige fat by targeting immuno-metabolic pathways.

Keywords: BMP4, fat browning, adipose tissue macrophages

Introduction

Obesity increases the risk of severe health consequences, including type 2 diabetes, cardiovascular diseases, and some types of cancer. Obesity is characterized by the excess accumulation of adipose tissue. It is commonly accepted that mammals possess two major types of adipose tissues: white adipose tissue (WAT) for storing energy and brown adipose tissue (BAT) for dissipating stored energy. Another kind of adipocyte with a high expression level of UCP1 was recently identified in WAT and is activated under circumstances, such as cold exposure and exercise (Cypess et al., 2009; van Marken et al., 2009; Virtanen et al., 2009; Bostrom et al., 2012; Wang et al., 2013). Due to its ability to dissipate energy, beige fat is regarded as a potential therapeutic target for obesity and diabetes.

Although beige and brown adipocytes have similar UCP1-dependent function, these cells differ from each other both developmentally and anatomically. The classical brown adipocytes arise from the same $Pax7^{+}Myf5^{+}$ precursor cells as myocytes (Seale et al., 2008; Kajimura et al., 2009), whereas beige adipocytes arise from a $Pax7^{-}Myf5^{-}$ lineage and are mostly present in subcutaneous WAT (scWAT) (Wu et al., 2012; Sanchez-Gurmaches and Guertin, 2014). The sympathetic nervous system releases the sympathetic neurotransmitter norepinephrine (NE) and plays a major role in the lipolysis and the activation of BAT in response to chronic cold exposure (Morrison et al., 2012). Upon cold exposure, BAT, which richly innervated by sympathetic fibres, promotes thermogenesis through the release of NE, whereas in WAT, with less innervated fibres, the beige adipocytes are still elicited (Kreier et al., 2002; Bartness et al., 2010). A range of small molecules and hormones are implicated in enhancing beige adipocytes, including irisin and meteorin-like (Metrnl) released by muscle (Bostrom et al., 2012; Rao et al., 2014), and IL-6 and PTH-related protein (PTHrP) elevated in cachexia patients (Kir et al., 2014; Petruzzelli et al., 2014).

Adipose tissue is composed of adipocytes, immune cells, and a vasculature, and thus, beiging is a process that involves the orchestration of a variety of cell types. Among these cells, macrophages are known for their multi-functions in inflammation, angiogenesis, tissue remodelling, and metabolism (Bapat et al., 2015). Macrophages participate in the activation of beige adipocytes. Upon cold challenge or exercise, elevated Metrnl stimulates the release of IL-4 by eosinophils, consequently increasing

Received October 13, 2017. Revised January 10, 2018. Accepted February 15, 2018.

the number of M2 macrophages, which stimulates the secretion of NE/catecholamines, leading to the activation of beige fat in WAT (Qiu et al., 2014; Rao et al., 2014). Although recent report argued that NE in macrophages was not sufficient to induce beiging (Fischer et al., 2017), data in other studies confirmed the beiging effect of M2 macrophage (Liu et al., 2014). It is also reported that the formation of beige fat, upon cold exposure, involves M2 macrophages that stimulated by cytokines, such as adiponectin (Hui et al., 2015). Since beiging is a complicated process that may be accompanied by the release of cytokines other than adiponectin, the potential function of these cytokines on macrophage regulation should be studied when exploring the mechanism of beige fat formation.

BMP4 is a secreted protein that performs its functions by binding to its receptors and activates the downstream signalling. Smads and p38/MAPK pathways are the two canonical pathways activated by BMP4 (Derynck and Zhang, 2003). BMP4 is a key regulator of mesoderm formation during the gastrulation stage of embryogenesis. However, in adults, BMP4 is highly expressed in adipose tissue and plays important roles in adipocyte development and metabolism. BMP4 not only commits stem cells to the adipose lineage but also regulates the metabolism of adipose tissue. The function of BMP4 in adipose metabolism is indicated by its elevated expression level after cold exposure and is evidenced by the results that WAT overexpressing BMP4 is induced to beige fat formation, which is characterized by a high expression of UCP1 in adipocytes, an enriched vasculature, and an elevated insulin sensitivity (Qian et al., 2013; Tang et al., 2016). Herein, we explored the potential role of BMP4 in beige fat formation through adipose tissue macrophages (ATMs). We found that the total ATMs and the M2/M1 ratio increased in the scWAT of BMP4 TG mice and decreased in BMPR2 KO mice. BMP4 activated M2 macrophages by promoting M2 macrophage proliferation, in which the p38/MAPK/STAT6/PI3K–AKT signalling pathway is involved. Meanwhile, BMP4 inhibited M1 macrophage activation. Importantly, BMP4-activated M2 macrophages had an improved ability to induce beige fat formation. Therefore, the induction of beige fat through BMP4-regulated ATMs may represent a new strategy to treat obesity.

Results

BMP4 signalling increases M2/M1 ratio of ATMs in scWAT

Previous studies show that BMP4 is highly expressed in WAT with its level being higher in mature adipocytes than in the stromal vascular fraction (SVF). Since BMP4 is a secretory protein, the overexpression of BMP4 (Supplementary Figure S1A) specifically in adipocytes led to the elevated level in serum (Supplementary Figure S1B). BMP4 may exert an effect on neighbouring macrophages in a paracrine manner and/or in an endocrine manner. To examine the role of BMP4 in the regulation of ATMs, including type 1 (M1) and type 2 (M2) cells, the SVF, in which ATMs are enriched, was isolated from the scWAT of 8-week-old wild-type (WT) and BMP4 overexpression transgenic (BMP4 TG) male mice by collagenase digestion. The proportion of the two types of macrophages was defined by $CD45^+F4/80^+CD11c^+$ (M1) or $CD45^+F4/80^+CD206^+$ (M2) using flow cytometry. The proportion of adipose M2 macrophages as well as total macrophages increased in the scWAT from the BMP4 TG mice compared to the WT mice (Figure 1A). On the other hand, the proportion of M1 macrophages was modestly reduced in the BMP4 TG mice (Figure 1A). As a result, the M2/M1 ratio increased in the BMP4 TG mice (Figure 1B). The changes in the expression patterns of the M1 and M2 markers in the SVF were also examined, and the M2 markers (Arg1, Retnla, and Pdcdilg2) were dramatically elevated in the BMP4 TG mice (Figure 1C), whereas the M1 markers (IL, Nos2, and TNFα) were deceased (Figure 1D), which was consistent with the changes in percentage of ATMs after BMP4 overexpression in the adipose tissue.

BMP4 exerts its effects via binding its specific type I and type II receptors and activating its downstream signalling. BMPR2 is the type II receptor in adipose tissue. Because BMPR2 knockout is driven by fatty acid binding protein 4 (FABP4), which is also expressed in macrophages, BMPR2 in the knockout model mouse was down regulated in the macrophages (Supplementary Figure S1C). Changes in the ATMs were determined to further verify the role of BMP4, and its signalling, in the regulation of the ATMs. BMPR2 knockout inhibited M2 macrophage activation, as shown by its reduced proportion by flow cytometry (Figure 1E) and the expression of the relative markers by real-time PCR (Figure 1G). By contrast, both the percentage and the characteristic gene expression of the M1 macrophages were enhanced (Figure 1E and H), and this change was accompanied by an obvious decrease in the M2/M1 ratio (Figure 1F). These results indicate that BMP4 regulates ATMs and leads to an increased M2/M1 ratio in scWAT.

BMP4 signalling stimulates M2 and inhibits M1 macrophages

To define whether BMP4 directly stimulates M2 macrophages or inhibits M1 macrophage activation, bone marrow-derived macrophages were treated with recombinant BMP4. The percentage of M1 or M2 macrophages was determined by flow cytometry, and the relative markers were examined by real-time PCR. Monocytes were first isolated from the bone marrow in the mouse tibia and were induced to differentiate into mature macrophages with M-CSF (Supplementary Figure S2A). After 7 days of induction, ~80% of the cells were F4/80 expressing macrophages, as confirmed by flow cytometry (Supplementary Figure S2B and C). Those cells were then polarized to M1 and M2 subtypes with LPS and IL-4, respectively (Supplementary Figure S2A). Approximately 60% of the cells were polarized into the M2 macrophage, as indicated by CD206 expression, and 78% cells transformed into M1 macrophages, as determined by CD11c expression (Figure 2A). BMP4 treatment during polarization increased the M2 proportion to 80% and its specific marker expression (Figure 2A and B) but decreased M1 proportion and expression of the relative markers (Figure 2C and D). Macrophages were also isolated from the mouse carrying the Loxp sequence at the BMPR2 site, and BMPR2 in cells were knocked down *ex vivo* by infection of adenovirus carrying Cre recombinase and LacZ as control. As expected, the M2 macrophage proportion significantly reduced from 64% in the LacZ group

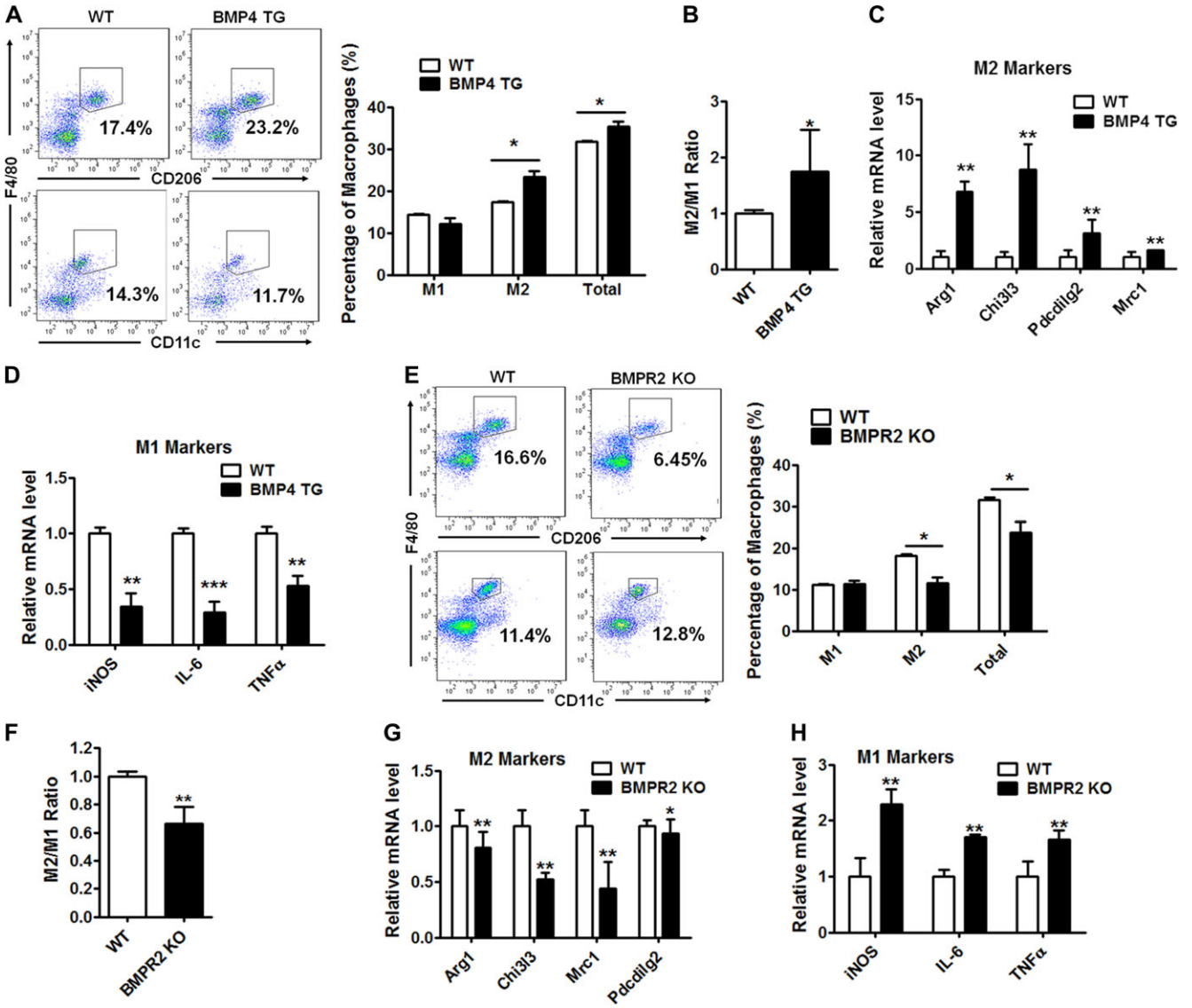

Figure 1 BMP4 signalling alters macrophage profile in the scWAT. (**A**) Flow cytometry analysis for M1 ($CD45^+F4/80^+CD11c^+$) and M2 ($CD45^+F4/80^+CD206^+$) macrophages in subcutaneous WAT (scWAT) from BMP4 transgenic (TG) and wild-type (WT) mice. $n = 6$. (**B**) M2/M1 ratio of macrophages in scWAT of WT and TG mice. $n = 6$. (**C** and **D**) M2 markers (Arg1, Chi3l3, Pdcdilg2, and Mrc1) and M1 markers (iNOS, IL-6, and TNFα) of macrophages in scWAT of WT and TG mice were determined by real-time PCR. $n = 3$. (**E**) Flow cytometry analysis for M2 and M1 macrophages in scWAT from BMPR2 knockout (KO) and control wild-type (WT) mice. $n = 14$. (**F**) M2/M1 ratio of macrophages in scWAT of WT and KO mice. $n = 14$. (**G** and **H**) M2 and M1 markers of macrophages in scWAT of WT and TG mice were determined by real-time PCR. $n = 3$. Data are presented as mean ± SD. Student's test was used for comparisons. $^*P < 0.05$; $^{**}P < 0.01$; $^{***}P < 0.001$.

to 46% in the BMPR2-knockdown group (Figure 2E), and the alteration was consistent with its specific marker expression (Figure 2F). On the other hand, the M1 macrophage proportion (Figure 2G) and its specific marker expression (Figure 2H) were elevated after BMPR2 was knocked down. These data suggested that BMP4 and its signalling through BMPR2 activated M2 macrophages and inhibited M1 macrophage activation.

BMP4 stimulates M2 macrophages proliferation

It is thought that tissue-resident M2 macrophages are maintained by local self-proliferation (Haase et al., 2014). However, M1 macrophages are more likely maintained by recruiting circulating monocytes to the adipose tissue (Lumeng et al., 2007a). To determine the way BMP4 regulates macrophages, the effect of BMP4 on cell proliferation was analysed by an EdU incorporation assay. Exogenous BMP4 was added into the medium at distinct stages of macrophage differentiation and polarization. The results showed that BMP4 obviously activated the proliferation of macrophages during the period of differentiation from monocytes (Figure 3A); ~21% of the cells were Edu positive after the BMP4 treatment compared to 8.7% Edu positive cells in the control (Figure 3B). Interestingly, pre-treating unpolarized macrophages

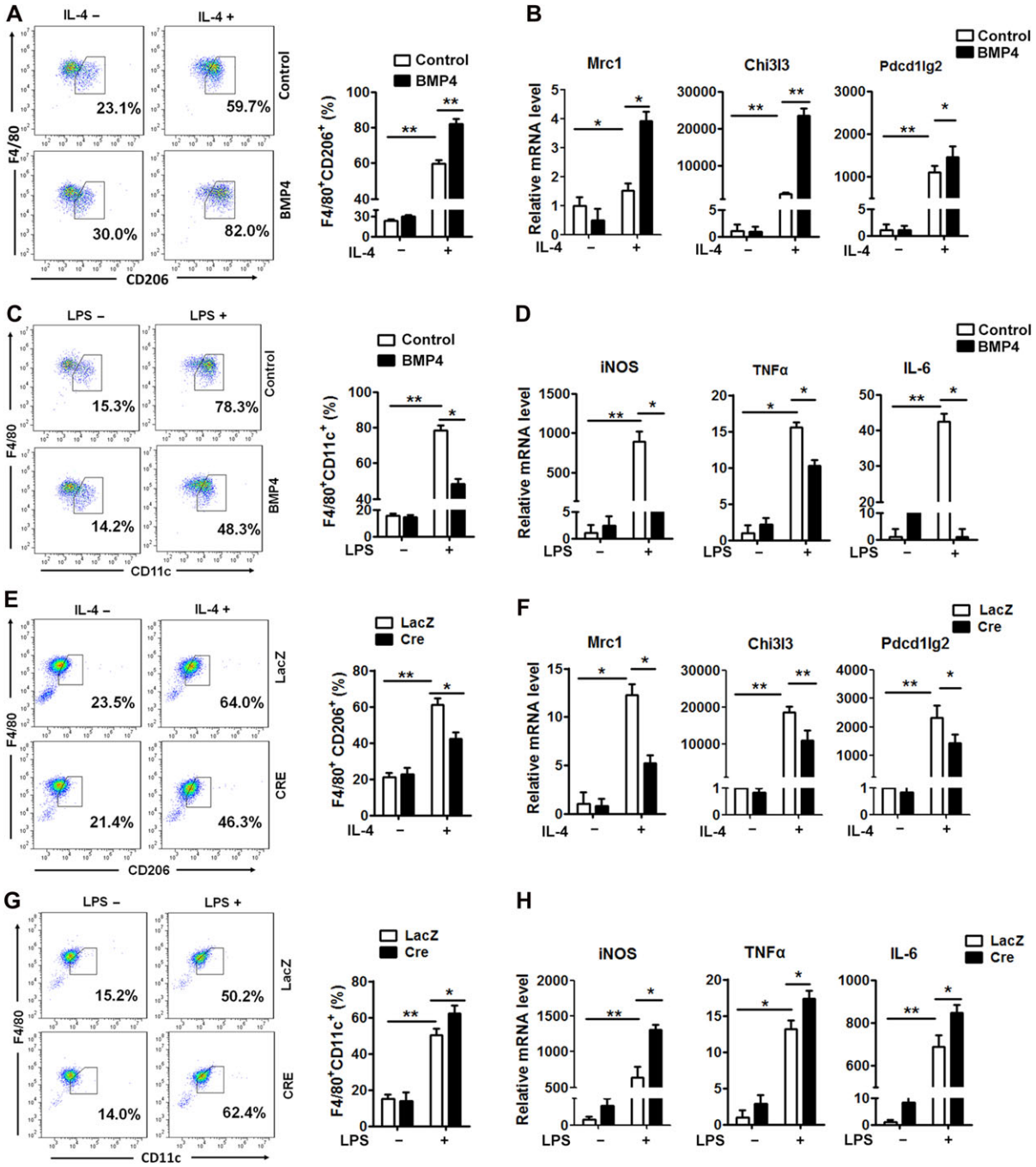

Figure 2 BMP4 signalling activates M2 and inhibits M1 macrophages. Monocytes isolated from bone marrow of tibias from WT or $BMPR2^{LoxP/LoxP}$ mice were cultured and induced with M-CSF to form macrophages, which were polarized to M2 and M1 cells by stimulation with IL-4 and LPS, respectively. Macrophages of $BMPR2^{LoxP/LoxP}$ genotype were infected with adenovirus carrying Cre recombinase or control LacZ to knockdown BMPR2 expression. (**A**) Flow cytometry analysis for proportion of M2 macrophage after BMP4 treatment. (**B**) Real-time PCR analysis for mRNA abundance of M2 macrophage markers, including Chi3l3, Pdcdilg2, and Mrc1 in cells treated as in **A**. (**C**) Flow cytometry analysis for proportion of M1 macrophage after BMP4 treatment. (**D**) Real-time PCR analysis for mRNA abundance of M1 macrophage markers, including iNOS, IL-6, and TNFα in cells referred in **C**. (**E**) Flow cytometry analysis for proportion of M2 macrophage in BMPR2 knockdown (Cre) and control (LacZ) groups. (**F**) Real-time PCR analysis for mRNA abundance of M2 macrophage markers, including Chi3l3, Pdcdilg2, and Mrc1 in cells referred in **E**. (**G**) Flow cytometry analysis for proportion of M1 macrophage in BMPR2 knockdown (Cre) and control (LacZ) groups. (**H**) Real-time PCR analysis for mRNA abundance of M1 macrophage markers, including iNOS, IL-6, and TNFα in cells referred in **G**. Data were collected from three individual experiments and presented as mean ± SD. Student's test was used for comparisons. $*P < 0.05$; $**P < 0.01$; $***P < 0.001$.

with BMP4 made the cells prone to form M2 macrophages (Figure 3C) but restrained them from forming M1 macrophages (Figure 3D). BMP4 also stimulated the proliferation of polarized M2 macrophages since the Edu positive cells show a more than 2-fold increase after BMP4 treatment (Figure 3E and F). However, BMP4 had no effect on proliferation of M1 macrophages (Figures 3E and F). Consistently, the mRNA expression of Ki67 was enhanced significantly in the M2 macrophages but was not in the M1 macrophages (Figure 3G). These data confirmed that BMP4 promoted the proliferation of M2 macrophages.

BMP4-stimulated M2 macrophage proliferation is regulated by the p38/MAPK/STAT6/PI3K–AKT pathway

To explore the mechanism by which BMP4 stimulates M2 macrophages proliferation, the differentially expressed genes between M2 macrophages with and without BMP4 treatment were analysed by RNA sequence. The signalling pathway analysis showed that molecules involved in phosphatidylinositide 3-kinase (PI3K) and AKT signalling were activated, which may be a response for M2 proliferation as reported (Ruckerl et al., 2012). p38/MAPK is one of the downstream factors of BMP4, and thus, we hypothesized that BMP4, and its downstream p38/MAPK, activates phosphor-AKT via STAT6 phosphorylation.

The western blot results showed that BMP4 caused a significant induction of p38/MAPK phosphorylation (Thr180/Tyr182) in the M2 macrophages, which was followed by the phosphorylation of STAT6 (Tyr641) and its downstream PI3K–AKT (Ser473) pathway. SB203580, an inhibitor of p38/MAPK, strongly blocked the effects of BMP4 on the pathway. Notably, in the M1 macrophages, the level of P-STAT6 was extremely low, and its

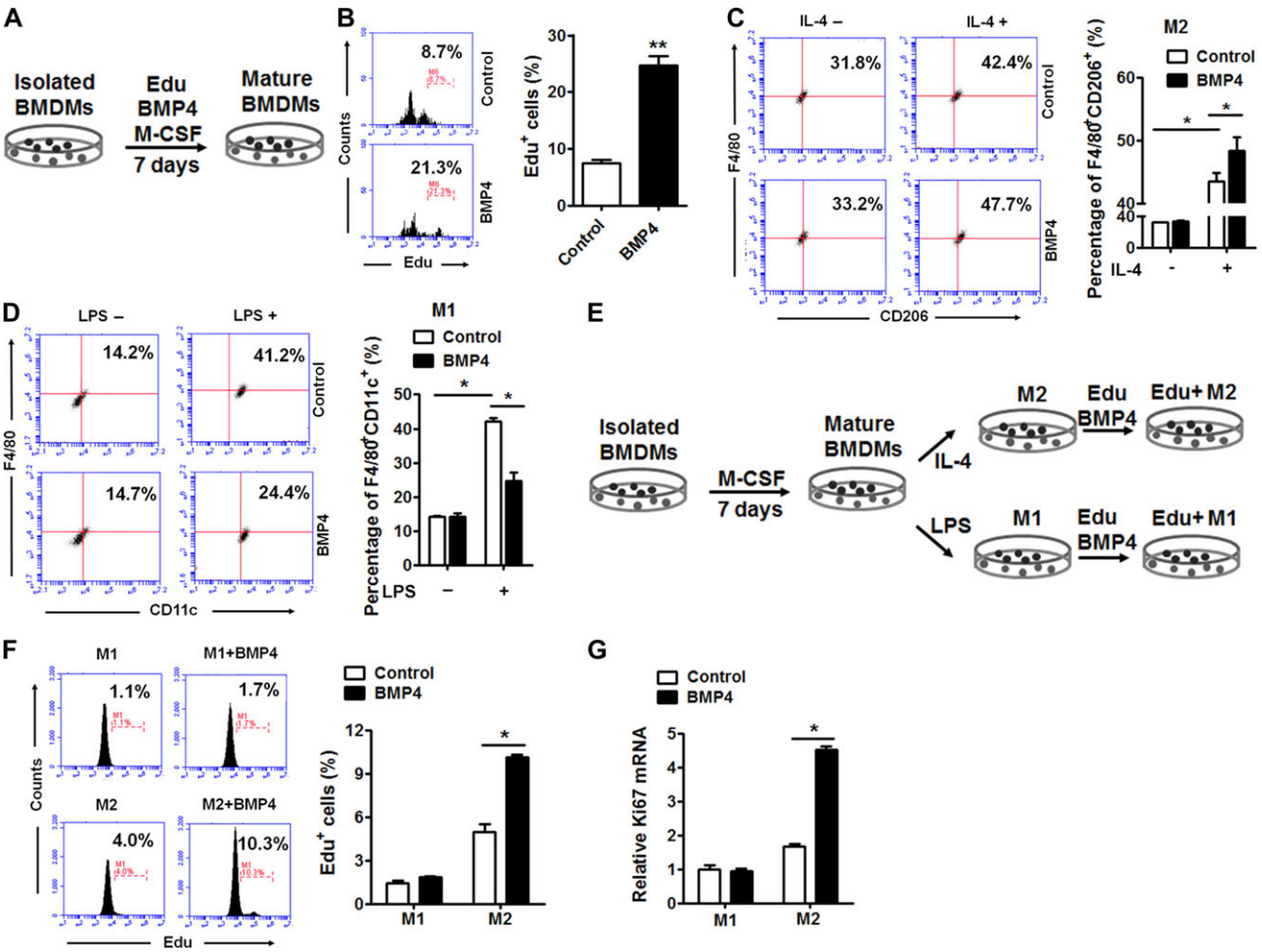

Figure 3 BMP4 promoted M2 macrophages proliferation *in vitro*. (**A**) Procedure of EdU incorporation into BMDMs: the BMDMs were differentiated into mature macrophages with M-CSF plus EdU with or without BMP4 treatment for 7 days. (**B**) Percentage of EdU^+ cells in BMDMs determined by flow cytometry. $n = 4$. (**C** and **D**) Flow cytometry analysis for M2 ($F4/80^+CD206^+$) (**C**, $n = 4$) or M1 ($F4/80^+CD11c^+$) (**D**, $n = 3$) macrophages with or without BMP4 treatment before polarization. (**E**) Procedure of EdU incorporation into M2 or M1 macrophages: the BMDMs were differentiated and polarized to M2 or M1 macrophages, followed by treatment of BMP4 plus EdU for 24 h before subject to flow cytometry analysis. (**F**) Flow cytometry analysis for EdU^+ M1 and M2 macrophages with or without BMP4 treatment. $n = 4$. (**G**) Quantitative real-time PCR showed mRNA levels of Ki67 in M1 and M2 macrophages with or without BMP4 treatment for 24 h. $n = 4$. Data were presented as mean ± SD. Student's test was used for comparisons. $^*P < 0.05$; $^{**}P < 0.01$; $^{***}P < 0.001$.

downstream P-AKT was not altered after the BMP4 treatment (Figure 4A). The knockdown of BMPR2 in the M1 and M2 macrophages from the BMPR2$^{LoxP/LoxP}$ mice by expressing Cre recombinase significantly diminished the expression of phospho-p38/MAPK (Thr180/Tyr182), which was followed a decrease in phosphor-STAT6 (Tyr641) and phosphor-AKT (Ser473) (Figure 4B). Although the knockdown of BMPR2 decreased the level of p38/MAPK in the M1 macrophages, it failed to decrease the level of P-AKT, which might be due to the low level of P-STAT6 (Figure 4B). However, BMP4 inhibited phosphorylated NFκB and phosphorylated JNK in M1

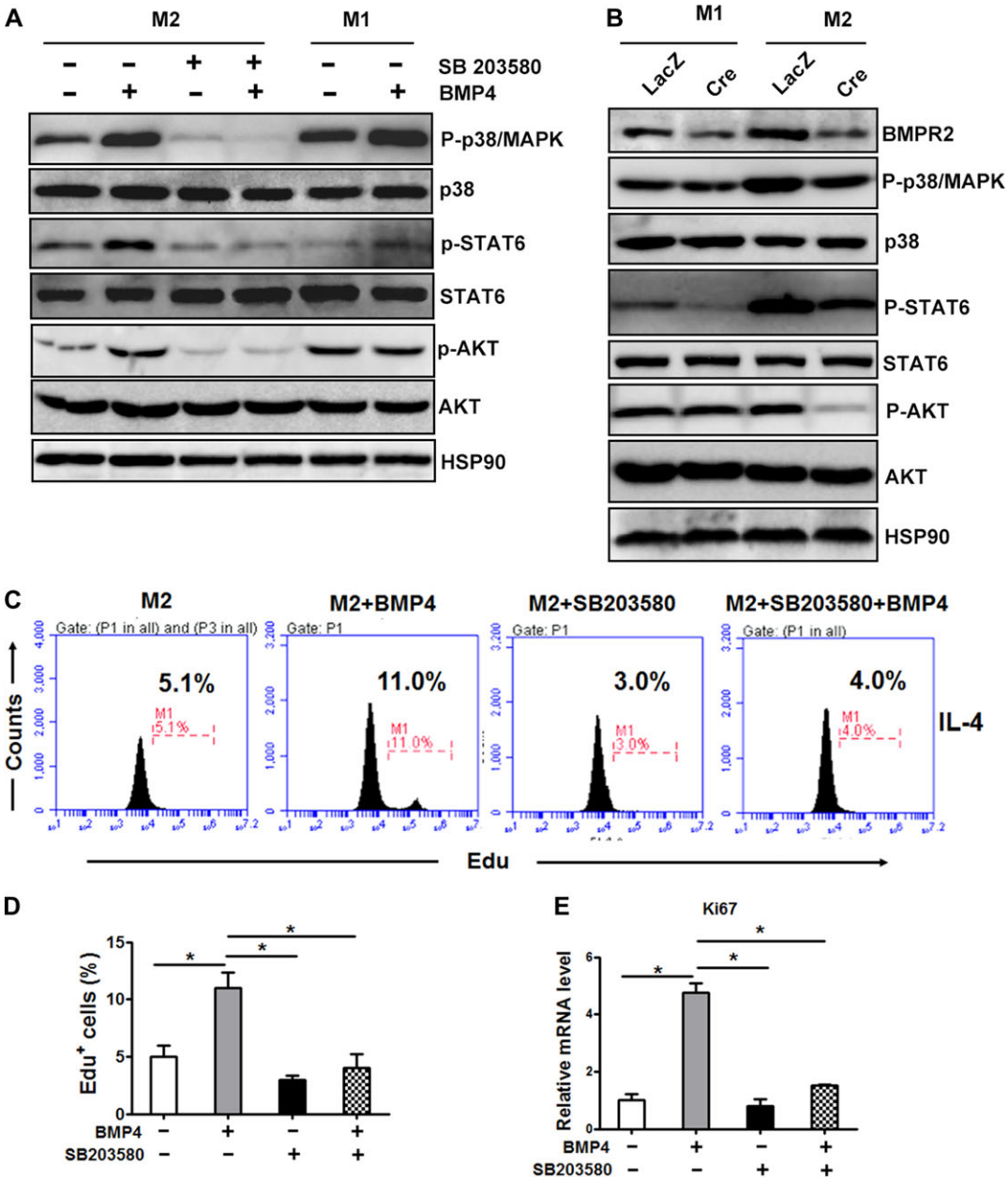

Figure 4 Activation of M2 macrophage is regulated by the p38/MAPK/STAT6/PI3K–AKT pathway. (**A**) Representative western blot images of the expression levels of molecules involved in the BMP signalling pathway in M2 and M1 macrophages treated with or without BMP4 (25 ng/ml) for 1 h. For p38 inhibition, cells were pretreated with p38 inhibitor SB203580 (20 nM) for 6 h. (**B**) Representative western blot images of molecules involved in the BMP signalling pathway in BMDMs derived from BMPR2$^{LoxP/LoxP}$ genotype mice and knocked down for BMPR2 by expressing Cre recombinase. (**C**) M2 macrophages were pre-incubated with the p38 inhibitor SB203580 (20 mM) for 6 h before addition of BMP4 (25 mg/ml). The amount of EdU^{+} macrophages was counted. (**D**) The quantification of EdU^{+} cells described in **C** from three individual experiments. (**E**) The mRNA levels of Ki67 in different groups of cells described in **C**. Data were collected from three individual experiments and presented as mean ± SD. Student's test was used for comparisons. *$P < 0.05$; **$P < 0.01$; ***$P < 0.001$.

macrophages, which might response for the inhibitive effect of BMP4 (Supplementary Figure S3). Furthermore, both flow cytometry analysis of the Edu incorporation (Figure 4C and D) and mRNA expression of Ki67 in the M2 macrophages (Figure 4E) demonstrated that pharmacological inhibition of p38/MAPK remarkably blocked the effects of BMP4 on M2 macrophage proliferation. Taken together, these findings suggested that the activation of the p38/MAPK/STAT6/PI3K–AKT pathway, induced by BMP4, played an important role in the proliferation of M2 macrophages.

BMP4 potentiates M2 macrophages to induce beige fat biogenesis

To explore the roles of BMP4-activated M2 macrophages in beige fat formation, we collected conditioned medium of M2 (M2-CM) and BMP4-treated M2 macrophages (BMP4-treated M2-CM) and used to incubate them with mature adipocytes differentiated from multipotent C3H10T1/2 stem cells for 2 days *in vitro* and examined their changes relating to beiging. Neither M2-CM nor BMP4-treated M2-CM changed the adipogenic differentiation of adipocytes as indicated by the expression level of C/EBPα and PPARγ (Supplementary Figure S4A). MitoTracker Green staining, which is manifested by active mitochondria, showed that the M2-CM indeed enhanced mitochondrial activity (Figure 5A). The results of Oil Red O staining for lipids also showed that the diameter of accumulated lipid droplets decreased after treatment with the M2-CM (Figure 5A), indicating the induction of catalytic lipid metabolism. Furthermore, western blot results showed that the expression of brown relative proteins, including UCP1, PGC1α, and PRDM16, increased (Figure 5B) along with genes indicating mitochondrial activities, including *Cyc S* and *COX2* and *COX4* by real-time PCR analysis (Figure 5C). Notably, the BMP4-treated M2-CM dramatically magnified the above changes induced by M2-CM (Figure 5A–C), indicating that BMP4 activated the M2 macrophages and enhanced their potential of inducing the beige function of adipocytes. The phenotypes were also observed in adipocytes differentiated from primary precursors isolated from subcutaneous adipose tissue (Supplementary Figure S4B). Some researchers reported that M2 macrophages activated beiging of adipocytes through NE, while Fischer K. and colleagues argued the effect of NE production by macrophages on beige cell activation. To explore whether BMP4-treated macrophage activates beige adipocytes is NE-dependent, we examined the expression of tyrosine hydrolase (TH) by real-time PCR in macrophages unpolarized, M2 macrophages polarized with IL-4, and BMP4-treated M2 macrophages. Expression of TH was generally low in macrophages. It was elevated when macrophages were induced to polarization by IL-4; however, BMP4 did not further increase

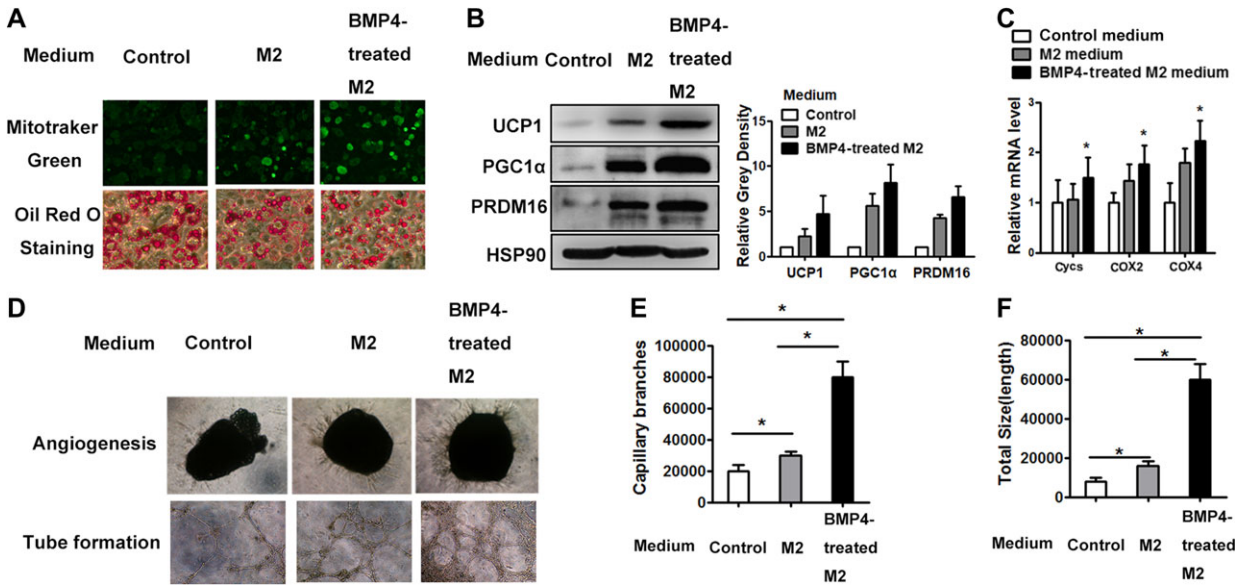

Figure 5 BMP4-treated M2 macrophages enhance beige cell activity and angiogenensis. Polarized M2 macrophages were induced with IL-4 after macrophage formation. Medium with BMP4 was added to the incubated M2 cells for 12 h and then washed out and changed with fresh medium for additional 12 h, which was collected as conditional medium. (**A**) Adipocytes differentiated from C3H10T1/2 were incubated with conditional medium for 2 days, followed by staining with Mito-tracker Green (upper panel) or Oil Red O (lower panel). (**B**) Western blot analysis of lysates (30 μg) of differentiated adipocytes for brown fat related gene expression. Relative gray intensity of bands from three individual experiments was quantified using Image J software. (**C**) Quantitative PCR showed mRNA levels of indicated genes of differentiated adipocytes from C3H10T1/2. $n = 3$. (**D**) Representative images of capillary sprouts of adipose tissue (upper panel) and tubes (lower panel) formed from SVF cells. (**E**) The quantitation of capillary branches from three individual experiments with Image Pro Plus. (**F**) The quantitation of tube length from three individual experiments with Image Pro Plus. Data were presented as mean ± SD. Student's test was used for comparisons. $^{*}P < 0.05$; $^{**}P < 0.01$; $^{***}P < 0.001$.

the expression of TH (Supplementary Figure S4D), which indicating other cytokines might play a role.

Increased angiogenesis is another key characteristic of beige fat, which adapts the tissue for a high metabolic rate. In the current study, an *ex vivo* angiogenesis assay was used to determine whether M2 and BMP4-treated M2 medium play a role in angiogenesis. The explants of scWAT, when exposed to M2-CM, developed more sprouts than that without the CM (Figure 5D and E). Furthermore, BMP4 activated the M2 macrophages and improved their potential to induce angiogenesis, as shown by the increased number capillary branches in this group (Figure 5D and E). The tube formation regulated by the M2 macrophages was also analysed using the SVF from inguinal fat. The quantitation of the total tube length revealed a strong increase if the incubating CM was derived from the BMP4-treated M2 macrophages (Figure 5D and F). The expression of cytokines related to the endothelium showed consistent changes with the tube length among the three groups (Supplementary Figure S4E). These data indicated that BMP4 stimulated angiogenesis by improving the potential of M2 macrophages to induce angiogenesis.

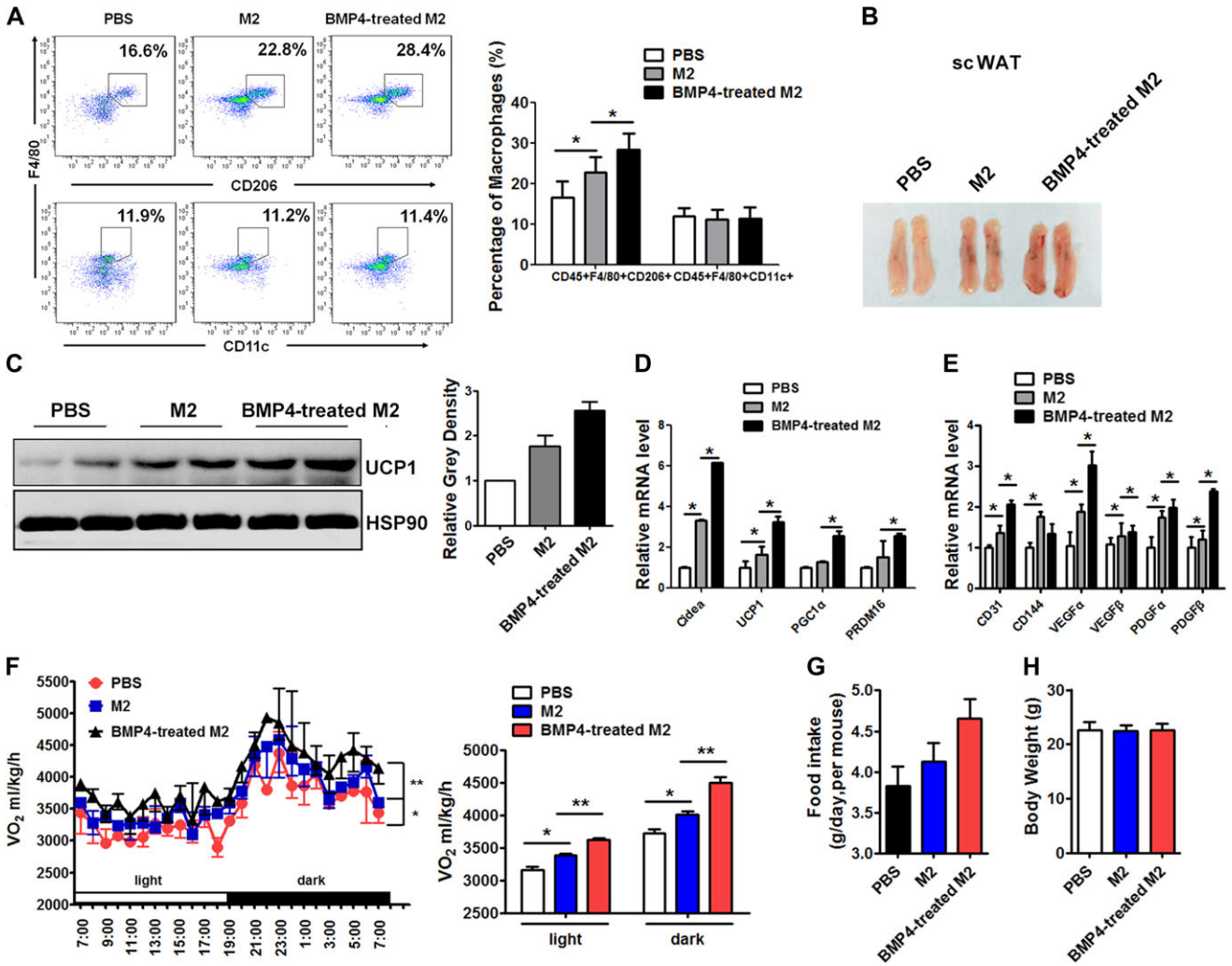

Figure 6 Adoptive transfer of BMP4-treated M2 promotes beige fat biogenesis and improves energy expenditure in mice. Eight-week-old male C57BL/6J mice housed at 22°C were adoptive transferred with 5×10^6 M2 macrophages or BMP4-activated M2 macrophages into each side of scWAT twice a week. Mice were examined after 2 weeks. (**A**) Flow cytometry analysis for the percentage of M1 macrophages ($CD45^+CD11c^+F4/80^+$) and M2 macrophages ($CD45^+CD206^+F4/80^+$) in scWAT transferred with macropahges. (**B**) Representative scWATs after transfer experiment. (**C**) Western blot analysis of UCP1 protein expression in scWAT. Relative gray intensity of bands from three individual experiments was quantified using Image J software. (**D**) Real-time PCR analysis for mRNA abundance of UCP1 and other markers for brown adipocytes, including Cidea, PRDM16, PGC1α, and UCP1. (**E**) Real-time PCR analysis for mRNA abundance of genes related to angiogenesis. (**F**) Whole-body oxygen consumption of three groups of mice were monitored in metabolic cage and calculated. (**G**) Daily food intake of mice during the period of adoptive transferred with M2 macrophages. (**H**) Body weight of mice in three groups maintained on chow diet after 2 weeks of adoptive transfer. Student's test was used and data are presented as mean ± SD $^*P < 0.05$; $^{**}P < 0.01$; $^{***}P < 0.001$. $n = 5$ mice per group.

Adoptive transfer of BMP4-stimulated M2 cells promotes beige fat biogenesis and improves energy expenditure in mice

The effects of BMP4-treated M2 macrophages on beige fat biogenesis *in vivo* were also investigated. Either 5×10^6 M2 macrophages or 5×10^6 BMP4-treated M2 macrophages were adoptively transferred into the scWAT of mice, and the transfer was performed twice a week. After 2 weeks, the population of macrophages was examined by flow cytometry. As shown in Figure 6A, the transfer of the M2 macrophages increased the proportion of M2 macrophages in the scWAT of the recipient mice. The M2 transfer did not alter the ratio of M1 macrophages ($CD45^+F4/80^+CD11c^+$). The percentage of M2 and M1 macrophages did not change after transfer in gonadal WAT (Supplementary Figure S5). The colour of the tissue appeared more reddish after the M2 injection and was even darker in the BMP4-treated M2 group (Figure 6B). Consistently, there was a marked induction of UCP1 protein in the scWAT of the mice injected with the M2 macrophages compared to the control mice (Figure 6C), which was enhanced by BMP4. This change was accompanied by an increase in the mRNA abundance of UCP1 and other markers for brown adipocytes, including *Cidea, PGC1α*, and *PRDM16* (Figure 6D), and genes for angiogenesis, such as VEGFα, VEGFβ, IGF, PDGFα, and PDGFβ (Figure 6E). Interestingly, although the number of transferred M2 cells and BMP4-treated M2 cells was same, the BMP4-treated M2 cells were more potent at enhancing the beiging of the WAT in the recipient WAT (Figure 6B–E).

To determine the effect of transferring the BMP4-treated M2 macrophages into the scWAT of the mice on their whole-body energy expenditure, oxygen consumption (VO_2) was monitored in metabolic cages, and the results were diverse among the adoptively transferred M2 macrophages and BMP4-treated M2 macrophages and the control PBS mice (Figure 6F). The mice receiving the transferred M2 macrophages displayed a significant elevation of oxygen consumption, while those receiving the transferred BMP4-treated M2 macrophages showed the highest level in VO_2, with an increased food intake that was not significant (Figure 6G). In contrast to the changes in the energy expenditure and food intake, body weight was not obviously altered by transferring the various cells (Figure 6H). Taken together, these findings suggest that BMP4 promotes the ability of M2 macrophages to facilitate beige fat formation.

Discussion

The interest in finding a way of promoting beige fat as a therapeutic target for obesity has risen recently. Several studies show that IL-4/AAMs play a significant role in regulating functional beige fat development in scWAT (Nguyen et al., 2011; Qiu et al., 2014; Rao et al., 2014). NE is thought to be released by AAMs, and acts to activate beige cell thermogenesis (Nguyen et al., 2011). More recently, M1 macrophages, which are dominant in the inflammation of adipose tissue, were also reported to play a role in the inhibition of beiging (Chung et al., 2017). Regarding the important role of macrophages in regulating the beiging, cytokines that acts on ATMs are worthy of exploration. BMP4 induces beiging of WAT—a process involves angiogenesis and increased thermogenesis in adipocytes (Sun et al., 2012; Sung et al., 2013; van den Berg et al., 2017). In this study, we found that BMP4 activates M2 and inhibits M1 macrophages, and the activated M2 macrophages promoted the thermogenic function of adipocytes as well as angiogenesis (Supplementary Figure S6). These results, together with our previous findings, might explain most of the events occurring in the beiging of WAT induced by BMP4.

A recent study reported by Fischer et al. (2017) showed that the deletion of TH expression and NE production in macrophages failed to impair thermogenesis of adipose tissue. However, the data did not exclude the role of M2 macrophages in energy metabolism, since most of the controls in their study were with M2 function included, which only suggested that there was no significant difference between macrophages with and without TH in activating beiging of adipocyte. They treated differentiated adipocytes with M2 macrophage conditioned medium for 6 h and found no changes in UCP1 and PGC1α expressions, while we extended the incubation time to 24 h and observed positive results with regard to the beiging-related adipocyte phenotype and gene expression. Thus, there should be other secreted factors function than NE—the one would expect changes within a very short time frame. While there are still no M2 macrophage-secreted hormone or cytokines identified, the secretary profile of M2 macrophages in beiging context deserves further study.

Macrophages are the most abundant immune cell population, accounting for 10%–40% in the lean and obesity states (Lumeng et al., 2007b). In the lean state, M2 macrophages predominate in the WAT and maintain the balance (Gordon 2003). In obesity, however, there is a major shift in the M1/M2 ratio due to the infiltration of M1 macrophages, while the number of M2 macrophages does not diminish (Lumeng et al., 2007a, b; Oh et al., 2012). In the present study, a significant reduction in the M1 macrophages was observed with the addition of exogenous BMP4 (Figure 2C), whereas such an effect was mild in the iWAT of the BMP4 TG mice (Figure 1A). One possible explanation is that the M2 macrophages dominate the resident population both in the BMP4 TG and BMPR2 KO mice, alleviating the changes of the M1 macrophage proportion. Interestingly, as for the source of the ATMs, circulating monocytes are recruited to the fat pad and polarize towards the classically activated form (Gordon and Taylor, 2005; Oh et al., 2012). Additionally, emerging evidence suggests that the *in situ* proliferation of M2 macrophages contributes to the predominance in the lean state. The accumulation of M2 macrophages in the iWAT after cold challenge is due to self-renewal instead of polarization from circulating monocytes (Lumeng et al., 2008). In the current study, BMP4 promoted M2 proliferation, leading to a dramatic elevation in M2 macrophages in the BMP4 TG mice (Figures 1A and 3C). The PI3K–AKT signalling pathway mediates the effects of IL-4 on M2 macrophage proliferation (Ruckerl et al., 2012). In the present study, we also detected the activation of components of PI3K–AKT signalling in the RNA sequence data and by western blot (Figure 4A). It is known that BMP4 activates p38/MAPK

pathway. After binding with BMP receptors, BMP4 activates transforming growth factor-β (TGF-β)-activated kinase 1 (TAK1)-binding protein 1. TAK1 is a member of MAPKKK family, which activates MKK3/MKK6. MKK3/MKK6 then activates p38/MAPK. P38/MAPK can also be activated by an MKK-independent mechanism achieved by autophosphorylation of p38 after interaction with TAK1 (Derynck and Zhang, 2003). The ability that p38/MAPK activates STAT6 has been demonstrated (Pesu et al., 2002; Jimenez-Garcia et al., 2015). As IL-4 activates STAT6 and PI3K–AKT when stimulating M2 macrophage, BMP4 enhanced the signalling of p38/MAPK/STAT3/PI3K–AKT was anticipated and evidenced in our cell model (Figure 4A). When inducing M1 macrophages, LPS elicits the activation of NFκB, and BMP4 have the inhibitive effect on NFκB activation (Supplementary Figure S3). As a result, BMP4 reduces the activation of M1 macrophage. The crosstalk between BMP4 and LPS signalling is similar to the report that BMP4 reduces expression and secretion of G-CSF by inhibiting NFκB activity in human and mouse tumour lines (Yamazaki et al., 2009).

We observed that transferring of M2 macrophages to subcutaneous region adjacent to fat pad activated beiging of subcutaneous adipose tissue and improved the metabolic rate of recipient mice, and BMP4-treated M2 macrophages were even more potent. However, what caused the improved effect by BMP4-treated M2 macrophages remained unresolved as the transferring of BMP4-treated M2 macrophages resulted in more M2 cells in fat pad. In addition to stimulating M2 macrophage proliferation (Figure 3F), the possibility that BMP4 changes the secretive profiles and makes M2 cells more potent in stimulating beiging of adipocytes will depend on the identification of specific cytokines, which deserves further exploration.

Beiging is a complicated process with multiple types of cells orchestrated to fulfil its function. In our present study, browning of the WAT accompanied by brown-like change of adipocytes, angiogenesis and increased O_2 consumption, could be promoted by BMP4 via M2 macrophages. These results suggest that macrophages have multiple confounding effect, which could be the basis for the increased energy expenditure and improved metabolism in FABP4-BMP4 transgenic mice observed in our previous work (Qian et al., 2013). This is especially important because although BMP4 was found to inhibit BAT (Modica et al., 2016; Hoffmann et al., 2017), its activity in beige fat still causes an increase in energy expenditure (Qian et al., 2013; Hoffmann et al., 2017).

In summary, the results of the present study show a new perspective role for BMP4 in promoting beige fat by regulating macrophages. In addition, the induction of beige fat through BMP4-activated M2 macrophages may represent the new strategy for targeting the immune system to treat obesity.

Materials and methods

Animals

FABP4-BMP4 TG mice were used in our previous study (Modica et al., 2016; Hoffmann et al., 2017). $BMPR2^{LoxP/LoxP}$ mice were generously provided by China Novartis Institutes for BioMedical Research Co. To generate mice with an adipocyte-specific knockout of BMPR2, $BMPR2^{LoxP/LoxP}$ were crossed with mice expressing Cre recombinase under the control of the adipocyte-specific promoter Fabp4 (Jackson Laboratory). Animals were housed on a 12-h light/dark cycle at 23°C with free access to water and food. Studies were performed in male BMP4 TG or BMPR2 KO mice and littermate controls. All studies were approved by Animal Care and Use Committee of the Fudan University.

Metabolic measurement

Indirect calorimetry was performed at 10 weeks age to measure whole-body VO_2. Briefly, mice were housed individually in metabolic cages (CLAMS, Columbus Instruments), acclimated for 48 h and maintained in a 12-h light/dark cycle. VO_2 measurement was recorded every 18 or 20 min for a 48-h period and normalized to its body mass.

Adoptive transfer assay

BMDMs were isolated and cultured according standard procedure. M2 macrophages were cultured with or without BMP4 for additional 24 h, and then enzymatically dissociated and collected. M2 or BMP4-treated M2 macrophages were injected into subcutaneous site adjacent to inguinal fat bilaterally with the same number of 5×10^6 at each side.

Isolation of bone marrow-derived macrophages

Bone marrow cells were isolated from the femur and tibia of 8-week-old C57BL/6 J mice and differentiated to mature macrophages for 7 days with DMEM containing 10% foetal bovine serum (FBS) and 10 ng/ml M-CSF, then changed to medium containing cytokine for 48 h to polarize cell to M1 (10 ng/ml LPS, Sigma) or M2 (10 ng/ml IL-4, Peprotech) before incubation with recombinant BMP4. For EdU incorporation, 5 mM EdU (Invitrogen) was added to the macrophages along with BMP4.

Flowcytomerty analysis of macrophages

SVF cells from iWAT and BMDMs were treated with PBS with 5% FBS for blocking and stained with fluorophore-conjugated antibodies or isotype control antibodies for 1 h and analysed with BD Accuri C6 (BD Bioscience). The antibodies used in these studies are F4/80-FITC (BioLegend), CD206-APC (BioLegend), CD45-PerCP (BD Bioscience), and CD11c-APC (BioLegend). For FACS analysis of EdU^+ cells, cells were analysed with the Click-it EdU Alexa Fluor 647 Flow Cytomentry Assay Kit (Life Technologies) according to the manufacturer's protocol.

Inguinal adipose tissue explants angiogenesis and tube formation

Explants from freshly harvested mouse inguinal adipose tissue were prepared into pieces of 1 mm^3 and embedded in growth factor reduced matrigel (BD Biosciences) on 96-well glass-bottom culture dishes (BD Biosciences). In brief, matrigel was allowed to polymerize at 37° for 15 min, followed with explants at 37° for 15 min, after which wells were filled with 100 μl EGM-2 media, and the media were replaced every other day. After 3 days of culture, the explants and the sprouting were recorded using Olympus

microscope. For tube formation assay, SVF cells at amount of 1×10^4/well/100 μl were plated on pre-casted Matrigel in 96-wells plate and incubated in EGM-2 media. After 6 h of culture, the formed tubes were either recorded using Olympus microscope or lysed with TRIZOL to prepare mRNA.

Statistical analysis

All data were expressed as mean ± SD. Statistical significance was determined by two-tailed Student's *t*-test. *P*-values of 0.05 or less were considered statistically significant (*$P < 0.05$; **$P < 0.01$; ***$P < 0.001$).

Supplementary material

Supplementary material is available at *Journal of Molecular Cell Biology* online.

Funding

This study was supported by grants from the National Natural Science Foundation of China (NSFC; 81390353 to Q.-Q.T., 31571471 to Q.-Q.T., and 31670787 to S.-W.Q.) and the Ministry of Science and Technology of China (MOST; 2013CB530601 to Q.-Q.T.).

Conflict of interest: none declared.

Author contributions:: S.-W.Q. and M.-Y.W. designed and conducted the experiments, analysed data, and wrote the manuscript. Y.-N.W., Y.-X.Z., and Y.Z. participated in conducting the experiments. Y.T. and Y.L. reviewed the manuscript and offered critical advice. L.G. participated in research discussion. Q.-Q.T. directed the project and reviewed the manuscript. Q.-Q.T. is the guarantor of this work and, as such, had full access to all the data in the study and takes responsibility for the integrity of the data and the accuracy of the data analysis.

References

Bapat, S.P., Myoung, S.J., Fang, S., et al. (2015). Depletion of fat-resident Treg cells prevents age-associated insulin resistance. Nature *528*, 137–141.

Bartness, T.J., Vaughan, C.H., and Song, C.K. (2010). Sympathetic and sensory innervation of brown adipose tissue. Int. J. Obes. *34(Suppl)*, S36–S42.

Bostrom, P., Wu, J., Jedrychowski, M.P., et al. (2012). A PGC1-α-dependent myokine that drives brown-fat-like development of white fat and thermogenesis. Nature *481*, 463–468.

Chung, K.J., Chatzigeorgiou, A., Economopoulou, M., et al. (2017). A self-sustained loop of inflammation-driven inhibition of beige adipogenesis in obesity. Nat. Immunol. *18*, 654–664.

Cypess, A.M., Lehman, S., Williams, G., et al. (2009). Identification and importance of brown adipose tissue in adult humans. N. Engl. J. Med. *360*, 1509–1517.

Derynck, R., and Zhang, Y.E. (2003). Smad-dependent and Smad-independent pathways in TGF-β family signalling. Nature *425*, 577–584.

Fischer, K., Ruiz, H.H., Jhun, K., et al. (2017). Alternatively activated macrophages do not synthesize catecholamines or contribute to adipose tissue adaptive thermogenesis. Nat. Med. *23*, 623–630.

Gordon, S. (2003). Alternative activation of macrophages. Nat. Rev. Immunol. *3*, 23–35.

Gordon, S., and Taylor, P.R. (2005). Monocyte and macrophage heterogeneity. Nat. Rev. Immunol. *5*, 953–964.

Haase, J., Weyer, U., Immig, K., et al. (2014). Local proliferation of macrophages in adipose tissue during obesity-induced inflammation. Diabetologia *57*, 562–571.

Hoffmann, J.M., Grunberg, J.R., Church, C., et al. (2017). BMP4 gene therapy in mature mice reduces BAT activation but protects from obesity by browning subcutaneous adipose tissue. Cell Rep. *20*, 1038–1049.

Hui, X., Gu, P., Zhang, J., et al. (2015). Adiponectin enhances cold-induced browning of subcutaneous adipose tissue via promoting M2 macrophage proliferation. Cell Metab. *22*, 279–290.

Jimenez-Garcia, L., Herranz, S., Luque, A., et al. (2015). Critical role of p38 MAPK in IL-4-induced alternative activation of peritoneal macrophages. Eur. J. Immunol. *45*, 273–286.

Kajimura, S., Seale, P., Kubota, K., et al. (2009). Initiation of myoblast to brown fat switch by a PRDM16-C/EBP-β transcriptional complex. Nature *460*, 1154–1158.

Kir, S., White, J.P., Kleiner, S., et al. (2014). Tumour-derived PTH-related protein triggers adipose tissue browning and cancer cachexia. Nature *513*, 100–104.

Kreier, F., Fliers, E., Voshol, P.J., et al. (2002). Selective parasympathetic innervation of subcutaneous and intra-abdominal fat—functional implications. J. Clin. Invest. *110*, 1243–1250.

Liu, P.S., Lin, Y.W., Lee, B., et al. (2014). Reducing RIP140 expression in macrophage alters ATM infiltration, facilitates white adipose tissue browning, and prevents high-fat diet-induced insulin resistance. Diabetes *63*, 4021–4031.

Lumeng, C.N., Bodzin, J.L., and Saltiel, A.R. (2007a). Obesity induces a phenotypic switch in adipose tissue macrophage polarization. J. Clin. Invest. *117*, 175–184.

Lumeng, C.N., DelProposto, J.B., Westcott, D.J., et al. (2008). Phenotypic switching of adipose tissue macrophages with obesity is generated by spatiotemporal differences in macrophage subtypes. Diabetes *57*, 3239–3246.

Lumeng, C.N., Deyoung, S.M., Bodzin, J.L., et al. (2007b). Increased inflammatory properties of adipose tissue macrophages recruited during diet-induced obesity. Diabetes *56*, 16–23.

Modica, S., Straub, L.G., Balaz, M., et al. (2016). Bmp4 promotes a brown to white-like adipocyte shift. Cell Rep. *16*, 2243–2258.

Morrison, S.F., Madden, C.J., and Tupone, D. (2012). Central control of brown adipose tissue thermogenesis. Front. Endocrinol. *3*, pii: 00005.

Nguyen, K.D., Qiu, Y., Cui, X., et al. (2011). Alternatively activated macrophages produce catecholamines to sustain adaptive thermogenesis. Nature *480*, 104–108.

Oh, D.Y., Morinaga, H., Talukdar, S., et al. (2012). Increased macrophage migration into adipose tissue in obese mice. Diabetes *61*, 346–354.

Pesu, M., Aittomaki, S., Takaluoma, K., et al. (2002). p38 mitogen-activated protein kinase regulates interleukin-4-induced gene expression by stimulating STAT6-mediated transcription. J. Biol. Chem. *277*, 38254–38261.

Petruzzelli, M., Schweiger, M., Schreiber, R., et al. (2014). A switch from white to brown fat increases energy expenditure in cancer-associated cachexia. Cell Metab. *20*, 433–447.

Qian, S.W., Tang, Y., Li, X., et al. (2013). BMP4-mediated brown fat-like changes in white adipose tissue alter glucose and energy homeostasis. Proc. Natl Acad. Sci. USA *110*, E798–E807.

Qiu, Y., Nguyen, K.D., Odegaard, J.I., et al. (2014). Eosinophils and type 2 cytokine signaling in macrophages orchestrate development of functional beige fat. Cell *157*, 1292–1308.

Rao, R.R., Long, J.Z., White, J.P., et al. (2014). Meteorin-like is a hormone that regulates immune-adipose interactions to increase beige fat thermogenesis. Cell *157*, 1279–1291.

Ruckerl, D., Jenkins, S.J., Laqtom, N.N., et al. (2012). Induction of IL-4Rα-dependent microRNAs identifies PI3K/Akt signaling as essential for IL-4-driven murine macrophage proliferation in vivo. Blood *120*, 2307–2316.

Sanchez-Gurmaches, J., and Guertin, D.A. (2014). Adipocytes arise from multiple lineages that are heterogeneously and dynamically distributed. Nat. Commun. *5*, 4099.

Seale, P., Bjork, B., Yang, W., et al. (2008). PRDM16 controls a brown fat/skeletal muscle switch. Nature *454*, 961–967.

Sun, K., Wernstedt, A.I., Kusminski, C.M., et al. (2012). Dichotomous effects of VEGF-A on adipose tissue dysfunction. Proc. Natl Acad. Sci. USA *109*, 5874–5879.

Sung, H.K., Doh, K.O., Son, J.E., et al. (2013). Adipose vascular endothelial growth factor regulates metabolic homeostasis through angiogenesis. Cell Metab. *17*, 61–72.

Tang, Y., Qian, S.W., Wu, M.Y., et al. (2016). BMP4 mediates the interplay between adipogenesis and angiogenesis during expansion of subcutaneous white adipose tissue. J. Mol. Cell Biol. *8*, 302–312.

van den Berg, S.M., van Dam, A.D., Rensen, P.C., et al. (2017). Immune modulation of brown(ing) adipose tissue in obesity. Endocr. Rev. *38*, 46–68.

van Marken, L.W., Vanhommerig, J.W., Smulders, N.M., et al. (2009). Cold-activated brown adipose tissue in healthy men. N. Engl. J. Med. *360*, 1500–1508.

Virtanen, K.A., Lidell, M.E., Orava, J., et al. (2009). Functional brown adipose tissue in healthy adults. N. Engl. J. Med. *360*, 1518–1525.

Wang, Q.A., Tao, C., Gupta, R.K., et al. (2013). Tracking adipogenesis during white adipose tissue development, expansion and regeneration. Nat. Med. *19*, 1338–1344.

Wu, J., Bostrom, P., Sparks, L.M., et al. (2012). Beige adipocytes are a distinct type of thermogenic fat cell in mouse and human. Cell *150*, 366–376.

Yamazaki, M., Fukushima, H., Shin, M., et al. (2009). Tumor necrosis factor α represses bone morphogenetic protein (BMP) signaling by interfering with the DNA binding of Smads through the activation of NF-κB. J. Biol. Chem. *284*, 35987–35995.